Exact breathing soliton solutions in combined time-dependent harmonic-lattice potential*

You Lu-Yun(佑六云)[a], Li Hua-Mei(李画眉)[a]†, and He Jun-Rong(何俊荣)[a][b]

[a] Department of Physics, Zhejiang Normal University, Jinhua 321004, China
[b] Department of Physics, Huazhong University of Science and Technology, Wuhan 430074, China

(Received 1 July 2013; revised manuscript received 10 September 2013; published online 24 January 2014)

We investigate the explicit novel localized nonlinear matter waves of the cubic-quintic nonlinear Schrödinger equation with spatiotemporal modulation of the nonlinearities and the harmonic-lattice potential using a modified similarity transformation. We also find that when the modulus of the Jacobian elliptic function in the limit closes to 1, the shapes of the breathing solitons may exhibit some interesting features, i.e., one breathing soliton dividing into two in the ground state. The stability of the exact solutions is investigated numerically such that some stable breathing soliton solutions are found.

Keywords: breathing soliton, cubic-quintic nonlinearity, harmonic-lattice potential

PACS: 05.45.Yv, 03.75.Lm, 42.65.Tg **DOI:** 10.1088/1674-1056/23/3/030501

1. Introduction

Bose–Einstein condensates (BECs)[1,2] operating in the linear regime loaded into the optical lattices (OLs)[3–7] can be used to reproduce phenomena well known in solid state physics, such as Bloch oscillations,[8,9] Landau–Zener tunneling,[10,11] and so on. A natural extension for BEC is to consider the effects of periodic time modulation of the OL potential on the stability of solitons. Suppression of leading order diffraction and the formation of subdiffractive solitons were realized in the time-dependent OL.[12,13] Moreover, it had been demonstrated that the strong periodical shaken OLs did not destroy the phase coherence of the BEC.[14]

An even more interesting property of OLs is that the periodic time-dependent lattice is accompanied by a harmonic confining potential. One shall refer to this potential as the combined harmonic-lattice potential. Harmonic-lattice potential may be realized in BECs by tuning the external magnetic field and the optically controlled interactions using the Feshbach resonance (FR) technique.[1,15,16] The dynamics of BEC solitons in the harmonic-lattice potentials have attracted extensive theoretical and experimental studies, such as, references [17]–[22] for the theory and numerics, references [23]–[25] for experiments, and reference [26] for a comprehensive review on BEC dynamics in static lattices.

It is feasible to investigate the dynamical properties of the BECs with spatially inhomogeneous interactions and the governing equation is a one-dimensional nonlinear Schrödinger equation (NLSE) with harmonic-lattice potential. During the past several years, many influential works have devoted to constructing exact analytical solutions of the NLSE.[3,27–31] It should be noted that, if two- and three-body interactions in BECs are considered, the NLSE should include the cubic and quintic (CQ) nonlinearities. However, there is a little work considering the cubic-quintic nonlinear Schrödinger equation (CQNLSE) in the time-dependent harmonic-lattice potential. Besides, so far, to our knowledge, the inhomogeneous physical models trapped in the harmonic-lattice potential are usually studied numerically, and the analytical results are rarely reported.

With the basis of this motivation in mind, in this paper, we investigate the explicit novel solutions of the CQNLSE with spatiotemporal modulation of the nonlinearities and the harmonic-lattice potential. We obtain breathing soliton solutions in terms of Mathieu and elliptic functions. In addition, the stability of the breathing solitons is investigated numerically.

The structure of this paper is as follows. In Section 2, the method and the solution procedure are present. In Section 3, the explicit novel localized nonlinear matter waves in terms of Mathieu and elliptic functions in the combined time-dependent harmonic-lattice potential are studied. In Section 4, the stability of the breathing soliton solutions is discussed. Finally, in Section 5, the conclusions are presented.

2. Theoretical model and its method

In this paper, we will choose the time-dependent harmonic-lattice potential

$$v(x,t) = f_1(t)x^2 + f_2(t)\cos[\omega_0\alpha(t)x], \tag{1}$$

where $f_1(t)$ denotes the strength of the harmonic potential term, $f_2(t)$ denotes the depth of the OL potential term, $\alpha(t)$

*Project supported by the National Natural Science Foundation of China (Grant Nos. 11175158 and 11374266) and the Natural Science Foundation of Zhejiang Province, China (Grant No. LY12A04001).

†Corresponding author. E-mail: lihuamei@zjnu.cn

© 2014 Chinese Physical Society and IOP Publishing Ltd

is a time-dependent function, x and t represent the spatial coordinate and time, respectively, and the parameter ω_0 is an arbitrary real constant.

We consider physical systems ruled by the CQNLSE, which can be written in the following dimensionless form:

$$\mathrm{i}\psi_t = -\psi_{xx} + v(x,t)\psi + g(x,t)|\psi|^2\psi + G(x,t)|\psi|^4\psi. \quad (2)$$

In the context of BECs, the complex function $\psi(x,t)$ represents the macroscopic wavefunction, $v(x,t)$ is an external potential determined by the expression (1), $g(x,t)$ and $G(x,t)$ are the inhomogeneous CQ nonlinear coefficients, corresponding to the two-body and three-body interactions, respectively. The symbols of $g(x,t)$ and $G(x,t)$ can be positive or negative, indicating that the interactions are repulsive or attractive, respectively. We focus on spatially localized solutions for which $\lim_{|x|\to\infty} \psi(x,t) = 0$.

To gain solutions of Eq. (2), we will use a modified similarity transformation[32]

$$\psi(x,t) = \sqrt{\alpha}Z(\xi)\Phi[X(x,t)] \times \exp\left[-\mathrm{i}\left(\frac{\alpha_t}{4\alpha}x^2 + \frac{\beta_t}{2\alpha}x - \gamma\right)\right], \quad (3)$$

where $X(x,t) = \int_{-\infty}^{\xi} Z[\xi'(x,t)]^{-2}\mathrm{d}\xi'$, $\xi = \alpha x + \beta$, $\alpha = \alpha(t)$, $\beta = \beta(t)$, and $\gamma = \gamma(t)$.

In the expression (3), $\Phi[X(x,t)]$ satisfies the stationary CQNLSE

$$\Phi_{XX} = -E\Phi + g_0|\Phi|^2\Phi + G_0|\Phi|^4\Phi, \quad (4)$$

where both $\Phi = \Phi(X)$ and $X = X(x,t)$ are real functions, E denotes the eigenvalue of the nonlinear equation and the real constants g_0 and G_0 control the CQ nonlinearities.

The substitution of Eq. (3) into Eq. (2) leads to Eq. (4), we obtain a set of equations about $g(x,t)$, $G(x,t)$, $v(x,t)$, and $Z(\xi)$. Solving these equations, we find the following solutions:

$$g(x,t) = g_0\alpha Z(\xi)^{-6}, \quad (5a)$$

$$G(x,t) = G_0 Z(\xi)^{-8}, \quad (5b)$$

where $Z(\xi)$ satisfies the Ermakov–Pinney equation[33]

$$Z_{\xi\xi} - B(\xi)Z = E/Z^3. \quad (6)$$

This equation has solution for $Z = Z(\xi)$ in the form

$$Z = \sqrt{Ay_1^2 + 2Cy_1y_2 + By_2^2}, \quad (7)$$

where A, B, and C are real constants satisfying $E = (AB - C^2)W^2$ and the Wronskian $W = y_1y_{2\xi} - y_2y_{1\xi}$ with $y_1 = y_1(\xi)$ and $y_2 = y_2(\xi)$ being two linearly independent solutions of the Mathieu equation

$$y_{\xi\xi} - B(\xi)y = 0. \quad (8)$$

In this paper, we choose $B(\xi) = 1 + \varepsilon\cos(\omega_0\xi)$, $\alpha = \sqrt{1+\varepsilon\cos(\omega_1 t)}$, $\beta = 0$, and $\gamma = \varepsilon\sin(\omega_1 t)/\omega_1 + t + \gamma_0$, where γ_0, ω_1, and $\varepsilon \in (-1,1)$ are arbitrary real constants, the solutions y_1 and y_2 can be expressed in terms of the Mathieu's C_{M} and S_{M} functions $y_1 = C_{\mathrm{M}}(-4/\omega_0^2, 2\varepsilon/\omega_0^2, \omega_0\xi/2)$ and $y_2 = S_{\mathrm{M}}(-4/\omega_0^2, 2\varepsilon/\omega_0^2, \omega_0\xi/2)$. We have the strength of the harmonic potential term

$$f_1(t) = \alpha_{tt}/4\alpha - \alpha_t^2/2\alpha^2, \quad (9a)$$

and the depth of the OL potential term

$$f_2(t) = \varepsilon\alpha^2. \quad (9b)$$

Such that the harmonic-lattice potential (1) is a combination of a time-modulated harmonic oscillator and an OL potential. Choosing some suitable parameters, the strength of the harmonic trap term $f_1(t)$, the depth of the OL term $f_2(t)$, and the harmonic-lattice potential are displayed in the Fig. 1. It is seen that they vary periodically with respect to time and are perfectly symmetric at each period.

Next, we will study the solutions of Eq. (2) obtained from the expression (3) via Eq. (4) and construct soliton solutions exhibiting interesting non-trivial behavior.

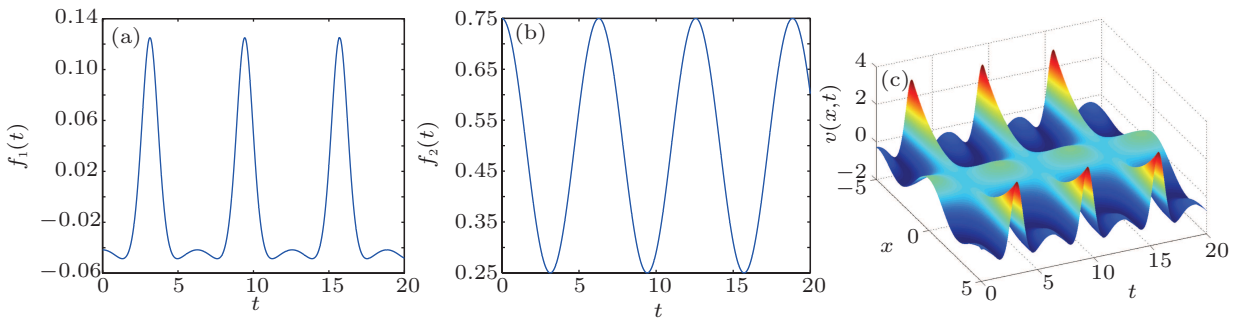


Fig. 1. (color online) (a) The strength of the harmonic trap term $f_1(t)$ and (b) depth of the OL term $f_2(t)$. (c) The examples of combined time-dependent harmonic-lattice potential $v(x,t)$. The other parameters are $\gamma_0 = 0$, $\omega_0 = 1$, $\omega_1 = 1$, and $\varepsilon = 0.5$.

3. Localized nonlinear waves in combined time-dependent harmonic-lattice potentials

3.1. Case of $E = 0$

If $E = 0$, the solution of Eq. (6) is a linear combination of the Mathieu functions[33]

$$Z = c_1 C_{\rm M}\left(-\frac{4}{\omega_0^2}, \frac{2\varepsilon}{\omega_0^2}, \frac{\omega_0\xi}{2}\right) + c_2 S_{\rm M}\left(-\frac{4}{\omega_0^2}, \frac{2\varepsilon}{\omega_0^2}, \frac{\omega_0\xi}{2}\right), \quad (10)$$

where constants c_1 and c_2 should be chosen to make Z sign-definite. Without the loss of generality, we set $c_1 = 1$ and $c_2 = 0$. This choice leads to

$$X(x,t) = \int_{-\infty}^{\xi} C_{\rm M}(-4/\omega_0^2, 2\varepsilon/\omega_0^2, \omega_0\xi'/2)^{-2}{\rm d}\xi'. \quad (11)$$

In fact, equation (4) possesses abundant exact solutions related to the different combinations of the different Jacobian elliptic functions. It is easy to prove that[34]

$$\Phi(X) = \frac{3{\rm sn}(\mu X, m)}{\sqrt{3a_0[3-(m^2+1){\rm sn}(\mu X, m)^2]}} \quad (12)$$

is an exact solution of Eq. (4) with $E = 0$, and

$$g_0 = -2/3a_0\mu^2(m^4 - m^2 + 1), \quad (13a)$$

$$G_0 = -1/9a_0^2\mu^2(m^2-2)(2m^2-1)(m^2+1), \quad (13b)$$

where a_0 is a constant and m is the modulus of the Jacobian elliptic function.

If we consider the boundary conditions $\psi(x \to -\infty) = \psi(x \to \infty) = 0$ for the localized solution, μ should satisfy

$$\mu[X(x \to \infty) - X(x \to -\infty)] = 2n{\rm K}(m), \quad (14)$$

where ${\rm K}(m) = \int_0^{\pi/2}[1 - m^2\sin^2\tau]^{-1/2}{\rm d}\tau$ is the complete elliptic integral of the first kind and $n = 1, 2, 3, \ldots$ is an integer number.

The expression (12) requires $a_0 > 0$, which gives $g_0 < 0$ for any m. From the expression (13b), we find that G_0 is negative for $0 < m < \sqrt{2}/2$ and positive for $\sqrt{2}/2 < m < 1$. Therefore, the cubic nonlinearity in the CQNLSE (2) can only be attractive, while the quintic can be either attractive or repulsive, depending on m. An exceptional point is remarkable for $m = \sqrt{2}/2$, since it gives $G_0 = 0$ and thus the quintic nonlinearity identically vanishes. Typical profiles of the nonlinearity modulations in the harmonic-lattice potential at $t = 0$ are displayed in the Fig. 2. It is seen that with a small m ($0 < m < \sqrt{2}/2$), the two-body and three-body interactions are both attractive and the cubic nonlinearities possess a larger amplitude, while for a large m ($\sqrt{2}/2 < m < 1$), the periodic quintic nonlinearity becomes positive, which means that the three-body interactions are repulsive, with a smaller amplitude. Figure 2 shows that no matter whether positive or negative of the CQ nonlinearities, the amplitude of the cubic nonlinearity is always larger than that of the quintic, which is rightly coherent to the fact that the two-body interaction in the dilute BEC is stronger than the three-body interaction.

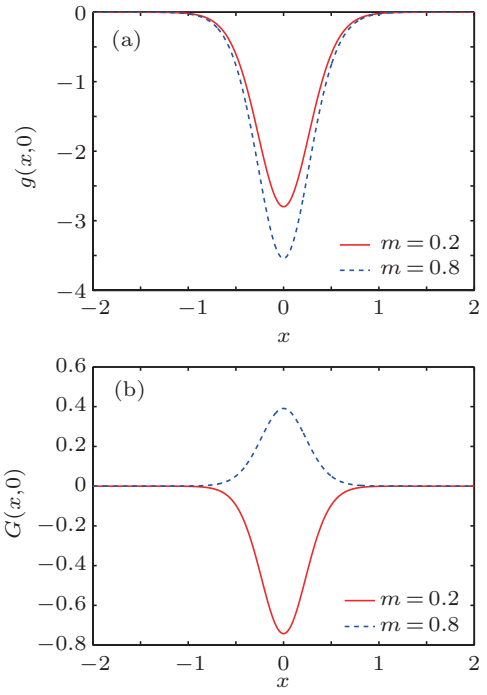


Fig. 2. (color online) (a) Examples of the inhomogeneous cubic nonlinear coefficient $g(x,0)$. (b) Examples of the inhomogeneous quintic nonlinear coefficient $G(x,0)$. The parameters are $a_0 = n = 1$ and $E = 0$. The other parameters are the same as those in the Fig. 1.

The expression (3) becomes

$$\psi_n(x,t) = \sqrt{\alpha}Z(\xi)\frac{3{\rm sn}(\mu X, m)}{\sqrt{3a_0[3-(m^2+1){\rm sn}(\mu X, m)^2]}} \times \exp\left[-{\rm i}\left(\frac{\alpha_t}{4\alpha}x^2 - \gamma\right)\right]. \quad (15)$$

By analyzing the expression (15), we find that the Mathieu functions $Z(\xi)$ have a minimum value at $\xi = 0$. In addition, when the elliptic modulus m becomes more and more close to 1 ($m \neq 1$), the shapes of the function $\Phi(X)$ have some changes, e.g., the sharp peak becomes more and more explanate with $n = 1$. Therefore, if $Z(\xi)$ is superimposed on $\Phi(X)$, through mathematical analysis, one obtains that for a bigger m ($m \to 1$ in the limit), the position of the peak develops into a small trough of wave in the ground state. This is still an interesting question, as unrealized in experiments, and will deserve separate studies. From Fig. 3(a), it can be seen that the larger the n, the larger the energy of the corresponding BEC state. Thus one may conclude that ψ_1 corresponds to the ground state and ψ_n corresponds to the $(n-1)$-th excited states. Figures 3(b) and 3(c) demonstrate the shapes of the localized stationary solutions (15) with different m. For a small elliptic modulus m, the peak of the ground state is tapering (see Fig. 3(b)); if m becomes more and more close to 1, the position of the peak

develops into a small trough of wave, which means that one wave crest splits into two wave crests ((see Fig. 3(c)).

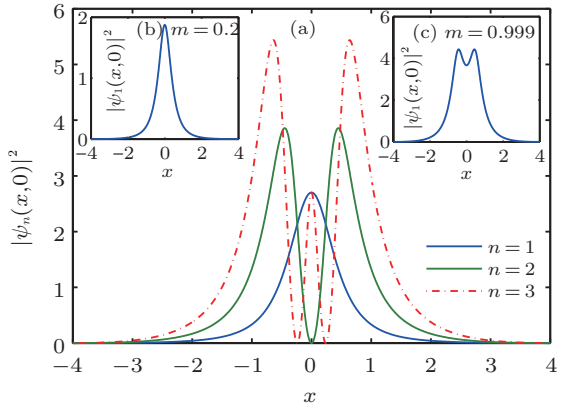


Fig. 3. (color online) Exact symmetric solitons (15) $\psi_n(x,0)$ for $m=0.8$ in the harmonic-lattice potential. (a) The blue solid line, green solid line, and red dashed-dotted line represent the solitons with $n=1$, $n=2$, and $n=3$, respectively. (b) The ground state soliton ($n=1$) with $m=0.2$. (c) The ground state soliton ($n=1$) with $m=0.999$. The other parameters are the same as those in the Fig. 2.

Adjusting the strength of the harmonic trap term $f_1(t)$ and the depth of the OL potential term $f_2(t)$ (see Figs. 1(a) and 1(b)), one can control the shapes of the localized nonlinear waves through the action of the harmonic-lattice management using the optical FR technique.

Next, we will research the dynamical properties of the localized nonlinear waves in the combined time-dependent harmonic-lattice potential (1). The variable $\xi = \sqrt{1+\varepsilon\cos(\omega_1 t)}x$ and the corresponding exact localized nonlinear waves can be obtained from the expression (15). Figures 4(a) and 4(b) describe the evolution of the density profiles for the wave function $\psi_n(x,t)$ in the harmonic-lattice potential with the parameter $m=0.2$. The density wave packets are localized in space and periodically oscillating in time, which are the so-called breathing solitons. Therefore, we construct some

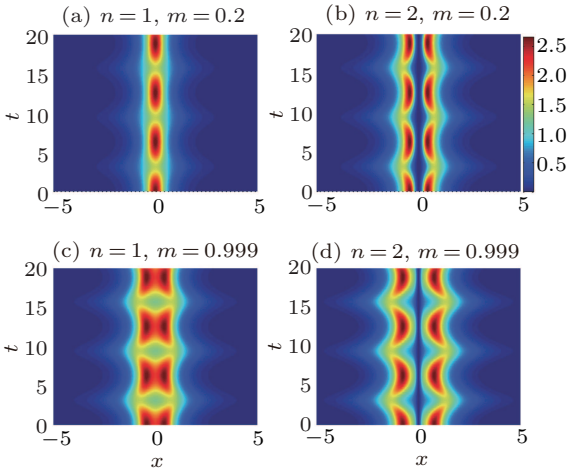


Fig. 4. (color online) Dynamics of the breathing solitons (15) in the combined time-dependent harmonic-lattice potential. (a) $n=1$, $m=0.2$; (b) $n=2$, $m=0.2$; (c) $n=1$, $m=0.999$; (d) $n=2$, $m=0.999$; The parameters are the same as those in the Fig. 2.

exact breathing n-soliton solutions of Eq. (2). In the Figs. 4(c) and 4(d), we display the breathing solitons for $m=0.999$. It is seen that the shapes of the breathing solitons may exhibit some interesting features, i.e., one breathing soliton dividing into two (see Fig. 4(c)).

3.2. Case of $E \neq 0$

If $E \neq 0$, the solution of Eq. (6) is given by expression (7). For simplicity, we choose $A=2$, $B=2$, and $C=0$, thus $E=4W^2$. The expression (7) becomes

$$Z=\sqrt{2y_1^2+2y_2^2}. \tag{16}$$

It is not difficult to verify that[34]

$$\Phi(X)=\frac{\mathrm{sn}(\mu X,m)}{\sqrt{a_0+a_1\mathrm{dn}(\mu X,m)^2}} \tag{17}$$

is a solution of Eq. (4) for $E\neq 0$, where

$$\mu=\sqrt{\frac{-E(a_0+a_1)}{2m^2a_1-m^2a_0-a_0-a_1}}, \tag{18}$$

$$g_0=\frac{2Em^2(a_0^2-2a_1a_0m^2-a_1^2+m^2a_1^2)}{m^2a_0+a_0-2a_1m^2+a_1}, \tag{19a}$$

and

$$G_0=\frac{3Ea_1a_0m^4(a_0+a_1-m^2a_1)}{m^2a_0+a_0-2a_1m^2+a_1}. \tag{19b}$$

In this case, the boundary condition is determined by the expression (14).

The inhomogeneous CQ nonlinear coefficients are

$$g(x,t)=g_0\alpha(2y_1^2+2y_2^2)^{-3}, \tag{20a}$$

and

$$G(x,t)=G_0(2y_1^2+2y_2^2)^{-4}. \tag{20b}$$

Here, the two-body interactions are always attractive and stronger, while the value of the m determines that the three-body interactions are repulsive or attractive.

The expression (3) becomes

$$\psi_n(x,t) = \sqrt{\alpha}Z(\xi)\frac{\mathrm{sn}(\mu X,m)}{\sqrt{a_0+a_1\mathrm{dn}(\mu X,m)^2}} \times \exp\left[-\mathrm{i}\left(\frac{\alpha_t}{4\alpha}x^2-\gamma\right)\right]. \tag{21}$$

The graph of some breathing solitons for integers $n=1$ and $n=2$ is shown in the Fig. 5.

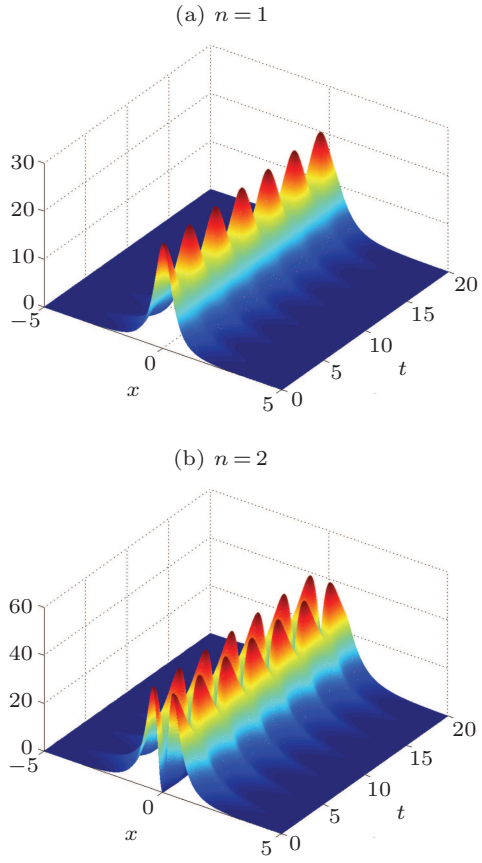


Fig. 5. (color online) Dynamics of the breathing solitons (21) in the combined time-dependent harmonic-lattice potential. (a) $n=1$; (b) $n=2$. The parameters are $m=0.2$, $A=B=2$, $C=0$, and $\omega_1=2$. The other parameters are the same as those in the Fig. 2.

4. Stability analysis

In this section, we perform some numerical simulations to the exact breathing solitons proposed in Section 3 by means of the split step Fourier-transform method.

Now, we add white noise in an initial pulse $\psi(x,0)$, i.e.,

$$\psi_{\text{pert}} = \psi(x,0)[1+0.01\text{random}(x)]. \tag{22}$$

We test the dynamical stability of the solution (15) by adding perturbation. Some results of numerical calculations are shown in Figs. 6 and 7(a). From Fig. 6, we find that the shapes of the breathing solitons show no change while evolving in time. Thus we can conclude that the solutions in the ground state are stable. Especially, when $m \to 1$, the soliton is still stable for $n=1$ (see Fig. 6(a)). From Fig. 7(a), it is observed that the breathing soliton with $n=2$ originally exhibits a quasistable evolution and then evolves into the one-way trace, when we add an initial white noise of level 1%. If $n>2$, one predicts the unstable soliton will quickly decay and so their structures are destructed. Besides, we have made numerical calculations for $E \neq 0$, and the results show that the breathing soliton solution (21) in the harmonic-lattice potential are unstable for all n.

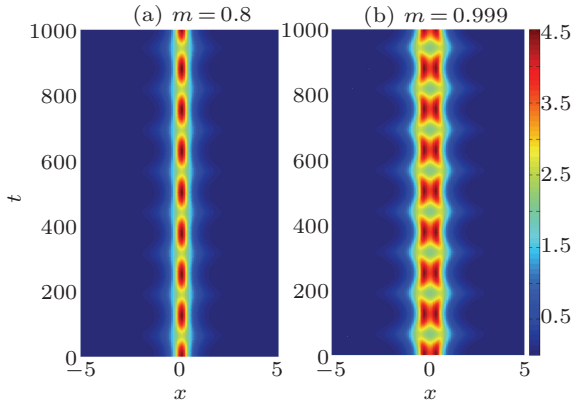


Fig. 6. (color online) Evolutions of stable breathing solitons (15) by adding perturbation with an initial white noise of level 1% for cases (a) with $m=0.8$ and (b) with $m=0.999$. The parameter is $n=1$ and the other parameters are the same as those in the Fig. 2.

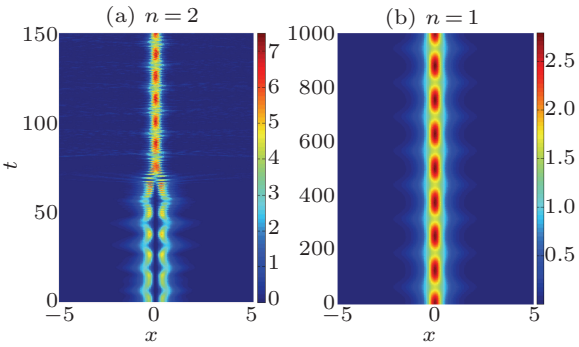


Fig. 7. (color online) (a) Evolution of unstable breathing soliton (15) by adding perturbation with an initial white noise of level 1%. (b) Numerical evolution of the breathing soliton (15) under the perturbation in the constraint conditions for parameter $G(x,t)=0.95G_0Z(\xi)^{-8}$. The parameter is $m=0.8$ and the other parameters are the same as those in the Fig. 2.

Next, we make a study for the perturbations in the constraint conditions (5), since it may be difficult to produce exactly such constraint conditions in real applications. Here, we take the breathing soliton solutions given by the expression (15) with $n=1$ as an example. It is found that when we perturb the constraint conditions in the way $g(x,t)=0.95g_0\alpha Z(\xi)^{-6}$ or $G(x,t)=0.95G_0Z(\xi)^{-8}$, and the other conditions do not change, the breathing soliton enters a stable state with time (see Fig. 7(b)).

5. Conclusions

In summary, by using the modified similarity transformation technique, we studied the explicit novel localized nonlinear matter waves of the CQNLSE with spatiotemporal modulation of the nonlinearities and the harmonic-lattice potential. By choosing the variable $X(x,t)$ as a appropriate integral form, some interesting properties of the breathing solitons have been analyzed and discussed. We also find that in the limit $m \to 1$, all the shapes of the solutions may exhibit some interesting features, i.e., one breathing soliton divides into two in the ground state. Finally we have checked the stability of the

breathing soliton solutions by employing the numerical split-step Fourier method. It is found that when $E = 0$, the breathing soliton in the combined time-dependent harmonic-lattice potential is stable for $n = 1$, by adding a white noise of level 1% in the initial pulse $\psi(x,0)$ or adding the perturbations in the constraint conditions (5). However, the excited states ($n > 1$) are all unstable. When $E \neq 0$, the breathing solitons are all unstable. We believe that the produce of designing nonlinearities and potentials will also be useful for the further study, such as, nonlinear optics, BECs, high-dimensional situations, more multicomponent systems, and so on.

References

[1] Inouye S, Andrews M R, Stenger J, Miesner H J, Stamper-Kurn D M and Ketterle W 1998 *Nature* **392** 151
[2] Pitaevskii L P and Stringari S 2003 *Bose–Einstein Condensation* (Oxford: Oxford University Press)
[3] Mayteevarunyoo T and Malomed B A 2006 *Phys. Rev. A* **74** 033616
[4] Poletti D, Alexander T J, Ostrovskaya E A, Li B and Kivshar Y S 2008 *Phys. Rev. Lett.* **101** 150403
[5] Theocharis G, Frantzeskakis D J, Carretero-González R, Kevrekidis P G and Malomed B A 2005 *Phys. Rev. E* **71** 017602
[6] Wang J D, Ji H and Liu P S 2013 *Chin. Phys. B* **22** 044207
[7] Tie L and Xue J K 2011 *Chin. Phys. B* **20** 120311
[8] Choi D I and Niu Q 1999 *Phys. Rev. Lett.* **82** 2022
[9] Cristiani M, Morsch O, Muller J H, Ciampini D and Arimondo E 2002 *Phys. Rev. A* **65** 063612
[10] Jona-Lasinio M, Morsch O, Cristiani M, Malossi N, Müller J H, Courtade E, Anderlini M and Arimondo E 2003 *Phys. Rev. Lett.* **91** 230406
[11] Jona-Lasinio M, Morsch O, Cristiani M, Malossi N, Müller J H, Courtade E, Anderlini M and Arimondo E 2004 *Phys. Rev. Lett.* **93** 119903
[12] Staliunas K, Herrero R and de Valcárcel G J 2006 *Phys. Rev. E* **73** 065603
[13] Staliunas K, Herrero R and de Valcárcel G J 2007 *Phys. Rev. A* **75** 011604
[14] Lignier H, Sias C, Ciampini D, Singh Y, Zenesini A, Morsch O and Arimondo E 2007 *Phys. Rev. Lett.* **99** 220403
[15] Roberts J L, Claussen N R, Burke J P, Greene C H, Cornell E A and Wieman C E 1998 *Phys. Rev. Lett.* **81** 5109
[16] Theis M, Thalhammer G, Winkler K, Hellwig M, Ruff G, Grimm R and Denschlag J H 2004 *Phys. Rev. Lett.* **93** 123001
[17] Schneider P I and Saenz A 2013 *Phys. Rev. A* **87** 052712
[18] Zhang R, Sapiro R E, Mhaskar R R and Raithel G 2008 *Phys. Rev. A* **78** 053607
[19] Hawk B N and Nathan K J 2007 *Phys. Rev. E* **75** 036214
[20] Plata J 2004 *Phys. Rev. A* **69** 033604
[21] He J R and Li H M 2013 *Chin. Phys. B* **22** 040310
[22] Ott H, de Mirandes E, Ferlaino F, Roati G, Türck V, Modugno G and Inguscio M 2004 *Phys. Rev. Lett.* **93** 120407
[23] Li Z W, Ma X M, Pang H and Li F S 2011 *J. Phys.: Condens. Matter* **23** 255701
[24] Eiermann B, Anker T, Albiez M, Taglieber M, Treutlein P, Marzlin K P and Oberthaler M K 2004 *Phys. Rev. Lett.* **92** 230401
[25] Blakie P B, Bezett A and Buonsante P J 2007 *Phys. Rev. A* **75** 063609
[26] Morsch O and Oberthaler M 2006 *Rev. Mod. Phys.* **78** 179
[27] Wu L, Li Lu, Zhang J F, Mihalache D, Malomed B A and Liu W M 2010 *Phys. Rev. A* **81** 061805
[28] Zhong W P, Belić M R and Xia Y Z 2011 *Phys. Rev. E* **83** 036603
[29] Tian Q, Wu L, Zhang J F, Malomed B A, Mihalache D and Liu W M 2011 *Phys. Rev. E* **83** 016602
[30] Li Z J, Hai W H and Deng Y 2013 *Chin. Phys. B* **22** 090505
[31] Wang J D, Ji H and Liu P S 2013 *Chin. Phys. B* **22** 044207
[32] Belmonte-Beitia J, Pérez-García V M, Vekslerchik V and Konotop V V 2008 *Phys. Rev. Lett.* **100** 164102
[33] Hawkins R M and Lidsey J E 2002 *Phys. Rev. D* **66** 023523
[34] Tang X Y and Shukla P K 2007 *Phys. Rev. A* **76** 013612